IET Smart Grid

Research Article

IET Journals
The Institution of Engineering and Technology

Distributed finite-time information discovery-based secondary restoration for islanded microgrids

eISSN 2515-2947
Received on 7th April 2019
Revised 24th October 2019
Accepted on 25th October 2019
E-First on 26th February 2020
doi: 10.1049/iet-stg.2019.0106
www.ietdl.org

Sonam Shrivastava[1], Bidyadhar Subudhi[2] ✉

[1]*School of Electrical Engineering, Vellore Institute of Technology, Vellore 632014, India*
[2]*School of Electrical Sciences, Indian Institute of Technology, Goa 401403, India*
✉ *E-mail: bidyadhar@iitgoa.ac.in*

Abstract: A new finite-time secondary voltage and frequency restoration scheme for an islanded microgrid (MG) is proposed in this study. All distributed generators (DGs) do not have access to the voltage and frequency reference value which makes their control more challenging. Therefore, a finite-time Information Discovery Scheme (IDS) is incorporated into the distributed secondary control scheme. The IDS provides local estimates of the global references of voltage and frequency for DGs in finite-time, and distributed control scheme uses this information to restore the voltage and frequency of MG to their reference values while accurately sharing the active power among the DGs in finite-time. The proposed control scheme is implemented on a sparse communication network and obviates the need for a central controller thereby reducing the risk of single-point-failure. The proof for finite-time restoration and restoration time upper-bound are derived using Lyapunov theory. The effectiveness of the proposed control scheme is verified through simulation of an MG test system in MATLAB/SimPowerSystem environment for sudden load variation and time-varying communication topology. The proposed control scheme supports plug and play capability and exhibits better convergence performance and disturbance rejection than the asymptotic controller based on neighbourhood tracking error.

1 Introduction

Renewable power generation is a good solution for resolving the environmental pollution problems associated with the traditional power grid based on non-renewable fossil fuels. A microgrid (MG) facilitates the integration of renewable energy sources (RESs) with the main grid thus results in a more intelligent and flexible power system [1]. MGs are the cluster of RESs, storage devices, and loads and they can operate either in grid-tied mode or switch to islanded mode because of the scheduled maintenance or disturbances [2]. The voltage and frequency of an MG are controlled by the main grid in the grid-tied mode. Once the MG is switched into the islanded mode, the voltage and frequency stability and accurate active power-sharing among the distributed generators (DGs) are disoriented. To address these problems, a hierarchical control structure has been presented in [3]. It comprises of inner control loops, primary, secondary, and tertiary controls. The primary control works in a decentralised manner and is implemented locally at each DG terminal using a droop control scheme [4]. The lowest control level in the hierarchy, droop-based primary control maintains voltage and frequency stability, after islanding, but leads to voltage and frequency deviations from their reference values [5]. These deviations are compensated by applying the secondary control level [6]. The tertiary control level deals with power flow and cost optimisation in an MG network. The secondary control has evolved from centralised to the distributed structure.

Conventionally, secondary control schemes include centralised, decentralised, and distributed configurations, from which the centralised one necessitates a complex bi-directional communication network and a central computing unit. Therefore, a centralised approach suffers from single-point-failure, computational burden and communication congestion [6–8]. Compared to the centralised technique, distributed control structure is implemented on a sparse communication network and improves scalability, flexibility, and stability of MG network [9–21].

Majority of the distributed control methods use the multi-agent consensus protocol, and achieve consensus over an infinite time horizon. The asymptotic convergence time limits the controller performance and cannot be used in finite-time applications such as the situations of continuous load change. In [9], feedback linearisation is used to convert distributed voltage control problem into a tracking synchronisation problem, but frequency control and active power-sharing were not considered. Also, the control scheme was dependent on the parameters of the MG. A consensus-based distributed voltage control is proposed in [10]. However, no comment was given on frequency and active power regulation. A secondary control strategy only for frequency restoration is presented in [11]. Both voltage and frequency regulation issues were addressed in [12] but the voltage restoration depends on MG parameters and active power response exhibits serious oscillations with load variation. In [13], secondary control is implemented using a distributed networked approach. However, it requires a complex communication structure where each controller shares information with all other controllers in the MG, which is quite similar to a centralised one. Also, stability analysis has been not presented for the proposed control approach. Simpson-Porco *et al*. [14] present a distributed-averaging-proportional–integral control scheme for reactive power-sharing, and voltage and frequency restoration are neglected. Nasirian *et al*. [15] propose a droop-free control scheme and makes the controller dependable entirely on a communication network, which when fails degrades the controller performance. An exponential fast asymptotic control approach for both voltage and frequency restoration is presented in [21], but the convergence time is not defined. In [22], a distributed power-sharing control scheme is presented, where the active power supply-demand balance is achieved while reducing the data communication. However, the frequency stability is achieved asymptotically in ∼3 s.

Recently, to accelerate the convergence rate, several finite-time control methods, based on consensus algorithm have been proposed in the literature [16–20]. In [16, 17], finite-time control is proposed only for frequency restoration. Zuo *et al*. [18] propose a finite-time controller for voltage and frequency restoration, but the latter depends on the MG system parameters. Wang *et al*. [19] propose a finite-time cooperative control for voltage and frequency, and active power regulation but are unable to establish upper-bound for the restoration time. A distributed model predictive control-based voltage restoration scheme is proposed in [20], but it

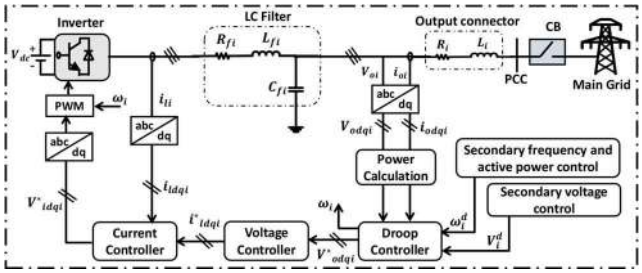

Fig. 1 *Dynamical model of inverter-based DG*

adopts asymptotic approach for frequency restoration and power-sharing. Following this line, in [23], a saturation function is exploited for finite-time frequency controller design to limit the control input within bound, but the voltage control method is realised via an asymptotic controller Similarly, Deng *et al*. [24] also present a finite-time bounded control scheme only for frequency and active power regulation. In [25], a low voltage distributed finite-time control approach is presented with an adaptive virtual impedance control to improve the active/reactive power-sharing accuracy.

In this paper, we proposed a finite-time distributed secondary control scheme for voltage, frequency, and active power regulation of an islanded MG. The upper-bound on the convergence time is derived via Lyapunov theory. In the distributed structure the DG units share the information with their neighbours only and do not have direct access to the reference. Hence, first, a finite-time information discovery scheme (IDS) is implemented in a distributed manner for each DG unit to obtain the local estimate of global reference information. Further, the proposed secondary control is implemented to achieve the voltage, frequency, and active power regulation in finite-time. The contributions of the proposed control scheme are as follows.

- Unlike the existing asymptotic convergence methods adopted in [9–15, 21], this paper proposes a finite-time control scheme for secondary voltage and frequency restoration and accurate active power-sharing.
- The global references for voltage and frequency are not always accessible for every DG unit present in the MG network. Thus, the proposed IDS combined with the proposed finite-time secondary control schemes provide accelerated convergence than the state-of-the-art approaches reported in [12, 16–19].
- The upper-bound on the convergence time is derived along with the stability proofs based on Lyapunov theory. Also, the restoration time does not depend on the MG parameters, i.e. line impedance, loads, and other DG parameters.
- The proposed control scheme is implemented on a sparse communication network and is fully distributed, and supports plug and play (PNP) capability of the MG. Also, in comparison with the distributed controller in [26], the proposed control scheme outperforms in terms of convergence time and accurate performance for sudden load variation and time-varying communication topology.

The rest of the paper is organised as follows. Section 2 provides the preliminaries on graph theory, primary control, and modelling of inverter-based DG unit. The proposed distributed finite-time frequency restoration and active power-sharing with the convergence stability proof are given in Section 3. Section 4 describes the finite-time distributed secondary voltage restoration. Finally, the simulation case studies to verify the efficacy of the proposed control scheme are given in Section 5. Section 6 concludes the paper.

2 Preliminary

Fig. 1 shows the block diagram of an inverter-based DG unit. It comprises a primary DC source interfaced with the MG bus via a voltage source inverter, LC filter, and an output connector. The inner control loop includes a droop controller, voltage, and current controller blocks. The detailed model description for the inverter-based DG can be found in [5].

2.1 Primary control analysis

The primary control level is employed locally at each DG terminal via a droop control scheme, to stabilise the voltage and frequency after islanding of the MG. For an MG consisting of N DG units, the voltage and frequency droop characteristics are given as

$$\omega_i = \omega_i^d - k_{Pi}^{\omega} P_i \tag{1}$$

$$V_{odi}^{*} = V_i^d - k_{Qi}^{V} Q_i \tag{2}$$

where V_{odi}^{*} is the output voltage magnitude, ω_i is the operating angular frequency, V_i^d and ω_i^d are the primary control voltage and frequency references set via the secondary controller, respectively. k_{Qi}^{V} and k_{Pi}^{ω} are the voltage and frequency droop coefficients for ith DG, respectively. The dynamics of the DG is derived in its own direct quadrature reference frame and making the quadratic term equal to zero. The primary control results in voltage and frequency deviations. Therefore, the aim of the secondary control level is to design the control scheme to restore the voltage and frequency to their references. The frequency control input ω_i^d solves the finite-time frequency restoration and the active power-sharing problem with restoration time T_f such that all DGs satisfy

$$\begin{cases} \lim\limits_{t \to T_f} (\omega_i - \omega_j) = 0, \quad \lim\limits_{t \to T_f} (k_{Pi}^{\omega} P_i - k_{Pj}^{\omega} P_j) = 0, \\ \omega_i = \omega_j = \omega_{\text{ref}}, \quad k_{Pi}^{\omega} P_i = k_{Pj}^{\omega} P_j, \quad \forall t \geq T_f, \quad \forall i, j \epsilon N \end{cases} \tag{3}$$

Further, the control input V_i^d solves the finite-time voltage restoration problem with settling time T_V such that all DGs satisfy

$$\begin{cases} \lim\limits_{t \to T_f} (V_{odi} - V_{odj}) = 0, \\ V_{odi} = V_{odj} = V_{\text{ref}}, \quad \forall t \geq T_V \quad \forall i, j \epsilon N \end{cases} \tag{4}$$

2.2 Graph theory

An MG network can be modelled as a directed graph represented as $G = (v_G, E_G, \boldsymbol{A}_G)$ with $v_G = \{1, 2, \ldots, N\}$ set of nodes (DG units), $E_G \subset v_G \times v_G$ is the set of edges (communication links) and $\boldsymbol{A}_G = [a_{ij}] \in R^{N \times N}$ is the associated adjacency matrix. a_{ij} is the weight of the edge (i, j), for $a_{ij} = 1$, ith node receives information from jth node, otherwise $a_{ij} = 0$. The Laplacian matrix of the graph G is $\boldsymbol{L}_G = \boldsymbol{D}_G - \boldsymbol{A}_G$, where $\boldsymbol{D}_G$ is the in-degree matrix defined as $\boldsymbol{D}_G = \text{diag}\{\boldsymbol{d}_i\}$, and diagonal matrix with $\boldsymbol{d}_i = \sum_{j \in N_i} a_{ij}$, i.e. number of incoming links at node i. The eigenvalues of $\boldsymbol{L}_G$ has at least one zero entry with all other have positive real parts and determines the global dynamics for the system [27].

3 Finite-time frequency restoration and active power-sharing

For the DGs, which do not have access to the reference value, the control becomes more complex and challenging. To overcome this problem, a finite-time IDS is used which is implemented locally at each DG unit to estimate the global reference value of frequency in finite-time t_{0f}. Further, the secondary control scheme is activated to restore the frequency deviation and achieve accurate active power-sharing in finite-time T_f.

3.1 Finite-time information discovery scheme for frequency

A sparse communication network is used for information sharing, and a direct connection to the leader node for each DG unit is unattainable. Only a subset of DG has access to the global reference values of voltage and frequency. To overcome this

problem a finite-time consensus-based information, discovery scheme can be designed as follows [28]:

$$\dot{x}_i = \mathrm{sig}\left(\sum_{j=1}^{N} a_{ij}(x_j - x_i) + c_i(\omega_{\mathrm{ref}} - x_i)\right)^{1/2} \tag{5}$$

where x_i is the local estimate of the global information ω_{ref}; $c_i \geq 0$ is the weight of the edge which has direct access to ω_{ref}; $\mathrm{sig}(z)^{\rho} = \mathrm{sgn}(z)|z|^{\rho}$ with $z \epsilon R, \rho > 0$; is the sgn function.

Remark 1: The observer designed in (5) guarantees that local frequency estimate terms x_i, $i = 1, 2, \ldots N$ synchronises to ω_{ref} in finite-time t_{of}, provided the communication network must be connected and $c_i \neq 0$ at least for one DG unit. To obtain the upper limit for the estimation time of IDS, define y_i under tracking synchronisation problem in continuous time as follows:

$$y_i = \sum_{j=1}^{N} a_{ij}(x_j - x_i) + c_i(\omega_{\mathrm{ref}} - x_i) \tag{6}$$

In the considered spare communication system, the information is received in discrete-time intervals and is updated after certain time interval, the discrete-time dynamics of the tracker synchronisation problem in (6) can be formulated as

$$\left\{ y_i(k) = \sum_{j=1}^{n} a_{ij}\big(x_j(k) - x_i(k)\big) - c_i(\omega_{\mathrm{ref}} - x_i(k)) \right. \tag{7}$$

where $x_i(k)$, $x_j(k)$, and $y_i(k)$ are the ith and jth DG voltages and the tracking control input at time instant k, respectively. $x_i(k+1)$ is the ith DG's state at time instant $(k+1)$ for next information update instant in discrete-time domain.

Here, we assume that the information is updated at equal periodic intervals. The tracking synchronisation control input in (7) can be written into a discrete matrix form as follows:

$$\boldsymbol{Y}(k+1) = -(\boldsymbol{L}_G + \boldsymbol{C}) + (\boldsymbol{x}(k) - 1_N \omega_{\mathrm{ref}}) \tag{8}$$

where $\boldsymbol{Y}(k+1) = [y_1(k+1), y_2(k+1) \ldots y_N(k+1)]^{\mathrm{T}}$; $\boldsymbol{x}(k) = [x_1(k), x_2(k) \ldots x_N(k)]^{\mathrm{T}}$; $\boldsymbol{C} = \mathrm{diag}(c_i)$ is a diagonal matrix; 1_N is Nth order vector with all entries equal to 1. Following Lemmas will be used to develop the main result.

Lemma 1: If the graph G is undirected and connected, then $(\boldsymbol{L}_G + \boldsymbol{C})$ is positive definite [18].

Lemma 2: The algebraic connectivity or second smallest eigenvalue of $\boldsymbol{L}_G(\boldsymbol{A}_G)$ is equal to [18]

$$\overset{\min}{\boldsymbol{x} \neq 0, 1_N^{\mathrm{T}}\boldsymbol{x}} \frac{\boldsymbol{x}^{\mathrm{T}}\boldsymbol{L}_G(\boldsymbol{A}_G)\boldsymbol{x}}{\boldsymbol{x}^{\mathrm{T}}\boldsymbol{x}} \geq \lambda_2(\boldsymbol{L}_G(\boldsymbol{A}_G))\boldsymbol{x}^{\mathrm{T}}\boldsymbol{x}\,.$$

Lemma 3: [29]*:* Let $\pi_1, \pi_2, \ldots, \pi_N \geq 0$ and $0 < p \leq 1\left(\sum_{i=1}^{N} \pi_i\right)^p \leq \sum_{i=1}^{N} \pi_i^p$

Lemma 4: Consider a continuous system $\dot{x} = f(x)$ with $f(0) = 0$. Suppose there exists a positive definite function $V: [0, \infty) \to [0, \infty)$, real numbers $l_1 > 0$, $0 < l_2 < 1$, such that $V \leq -l_1 V^{l_2}$. Then, V reaches zero in finite settling time [30]

$$T \leq \frac{V(x(0))^{1-l_2}}{l_1(1-l_2)}\,. \tag{9}$$

Theorem 1: Suppose that the graph G is connected and $c_i \neq 0$, for at least one DG. Under the distributed finite-time IDS in (6), the local estimate term x_i of each DG unit synchronises to ω_{ref} in finite-time given by (9).

Proof: Consider the Lyapunov function as

$$V_1(k) = e^{\mathrm{T}}(k)(I_N \otimes P)e(k) \tag{10}$$

where $e(k) = \left[e_1^{\mathrm{T}}(k), e_2^{\mathrm{T}}(k) \ldots e_N^{\mathrm{T}}(k)\right]^{\mathrm{T}}$ and

$$e_i(k) = x_i(k) - \frac{1}{N}\sum_{j=1}^{n} x_j(k) \tag{11}$$

is the error variable at time instant k. Now taking the values of $V_1(k)$ at the infinite sequence $k = 0, 1, \ldots$ from the view of time scale t we can get

$$\begin{aligned} V_1(k+1) - V_1(k) &= \sum_{l=0}^{m_k - 1}\left[V_1^{l+1}(k) - V_1^{l}(k)\right] \\ &= \sum_{l=0}^{m_k - 1}\left[\int_{k^l}^{k^{l+1}} \dot{V}_1(k)\,\mathrm{d}k\right] \end{aligned} \tag{12}$$

where $V_1^l(k)$ is the Lyapunov function in the discrete tie domain where $l = 0, 1, \ldots, m_k$, $k = 0, 1, \ldots$. Also, it is assumed that the continuous function $V_1(t)$ is continuously differentiable at any time except switching instances.

Remark 2: Differentiating continuous Lyapunov function

$$V_1(t) = \sum_{j=1}^{N}\int_0^{y_i} \mathrm{sig}(z)^{1/2}\,\mathrm{d}z \tag{13}$$

along the trajectory of (11), in between the information updating interval $(k+1)$ and k assuming it as a continuous function is equivalent to the difference $V_1(k+1) - V_1(k)$ in the discrete time domain.

From Remark 2 differentiating (13) with respect to time in continuous time domain we can get

$$\begin{aligned} \dot{V}_1(t) &= \sum_{j=1}^{N} \mathrm{sig}(y_i)^{1/2} \cdot \dot{y}_i \\ &= -\mathrm{sig}\left(\boldsymbol{Y}^{\mathrm{T}}\right)^{1/2}(\boldsymbol{L}_G + \boldsymbol{C})\mathrm{sig}(\boldsymbol{Y})^{1/2} \end{aligned} \tag{14}$$

From Lemma 1, $(\boldsymbol{L}_G + \boldsymbol{C})$ is positive definite until $c_i \neq 0$ for at least one DG. $\lambda_1(\boldsymbol{L}_G + \boldsymbol{C})$ is the smallest eigenvalue of $(\boldsymbol{L}_G + \boldsymbol{C})$ and is equal to $\lambda_2(\boldsymbol{L}_G)$. For $V_1 = 0$, $\boldsymbol{Y} = 0$, we can write

$$\dot{V}_1(t) = \frac{-\mathrm{sig}\left(\boldsymbol{Y}^{\mathrm{T}}\right)^{1/2}(\boldsymbol{L}_G + \boldsymbol{C})\mathrm{sig}(\boldsymbol{Y})^{1/2}}{\mathrm{sig}\left(\boldsymbol{Y}^{\mathrm{T}}\right)^{1/2}\mathrm{sig}(\boldsymbol{Y})^{1/2}} V_1^{2/3}(t)$$
$$\frac{\mathrm{sig}\left(\boldsymbol{Y}^{\mathrm{T}}\right)^{1/2}\mathrm{sig}(\boldsymbol{Y})^{1/2}}{V_1^{2/3}(t)}$$

Using Lemma 2, we can write

$$\dot{V}_1(t) \leq -\lambda_1(\boldsymbol{L}_G + \boldsymbol{C})V_1^{2/3}\frac{\mathrm{sig}\left(\boldsymbol{Y}^{\mathrm{T}}\right)^{1/2}\mathrm{sig}(\boldsymbol{Y})^{1/2}}{V_1^{2/3}(t)} \tag{15}$$

Further, $\mathrm{sig}\left(\boldsymbol{Y}^{\mathrm{T}}\right)^{1/2}\mathrm{sig}(\boldsymbol{Y})^{1/2} = \sum_{i=1}^{N}|y_i|$, and solving the third term in right-hand side of (15) the following can be obtained:

$$\frac{\mathrm{sig}\left(\boldsymbol{Y}^{\mathrm{T}}\right)^{1/2}\mathrm{sig}(\boldsymbol{Y})^{1/2}}{V_1^{2/3}(t)} = \frac{\sum_{i=1}^{N}\left|y_i\right|}{\left(\sum_{i=1}^{N}(2/3)\left|y_i\right|^{3/2}\right)^{2/3}} \tag{16}$$

Now using Lemma 3, (16) can be rewritten as follows:

$$\frac{\operatorname{sig}\left(\boldsymbol{Y}^{\mathrm{T}}\right)^{1/2}\operatorname{sig}(\boldsymbol{Y})^{1/2}}{V_1^{2/3}(t)} \geq \frac{\sum_{i=1}^{N}\left|y_i\right|}{\sum_{i=1}^{N}(2/3)^{2/3}\left|y_i\right|} \tag{17}$$

From (15) and (17), we can get

$$\dot{V}_1(t) \leq -\lambda_1(\boldsymbol{L}_G+\boldsymbol{C})\left(\frac{3}{2}\right)^{2/3} V_1^{2/3}(t) \leq 0 \tag{18}$$

Equation (18) resembles the negative definite function taken in Lemma 4. Hence, the estimated frequency term x_i of each DG synchronises to ω_{ref} in finite-time given as

$$t_{0f} \geq \frac{V(0)^{(1-q)}}{p(1-q)} \geq 3V_1(0)^{1/3}\lambda_1(\boldsymbol{L}_G+\boldsymbol{C}) \tag{19}$$

This completes the proof. □

3.2 Secondary frequency and active power regulation

To achieve the frequency restoration and accurate active power-sharing among DGs, the following control inputs are designed by differentiating (1) as follows:

$$\dot{\omega}_i = \dot{\omega}_i^d - k_{Pi}^{\omega}\dot{P}_i = \varepsilon_i^{\omega}, \quad \dot{\omega}_i^d = \varepsilon_i^{\omega} + k_{Pi}^{\omega}\dot{P}_i \tag{20}$$

For accurately sharing the active power define $k_{Pi}^{\omega}\dot{P}_i = \varepsilon_i^P$, and the frequency and active power control input can be given as

$$\omega_i^d = \int\left(\varepsilon_i^{\omega} + \varepsilon_i^P\right)\mathrm{d}t \tag{21}$$

The auxiliary control input ε_i^{ω}, and ε_i^P are designed as

$$\varepsilon_i^{\omega} = \alpha_{\omega}\sum_{j=1}^{N} a_{ij}\operatorname{sig}\left(\omega_j-\omega_i\right)^m + \beta_{\omega}\operatorname{sig}(\omega_{\mathrm{ref}}-\omega_i)^n, \quad t \geq t_{0f} \tag{22}$$

$$\varepsilon_i^P = \alpha_P\sum_{j=1}^{N} a_{ij}\operatorname{sig}\left(k_{Pj}^{\omega}P_j - k_{Pi}^{\omega}P_i\right)^q$$

where α_{ω}, β_{ω}, and α_P are the coupling gains, $0<m<1$, and $n=(2m/(m+1))$. Define $\delta_{\omega i}=\omega_i-\omega_{\mathrm{ref}}$, and $\dot{\delta}_{\omega i}=\dot{\omega}_i$, and $\delta_{Pi}=k_{Pi}^{\omega}P_i-(1/N)\sum_{i=1}^{N}k_{Pi}^{\omega}P_i$. Since $(1/N)\sum_{i=1}^{N}k_{Pi}^{\omega}\dot{P}_i=0$ for an non-directed network thus, $(1/N)\sum_{i=1}^{N}k_{Pi}^{\omega}P_i$ is time invariant, and $\dot{\delta}_{Pi}=k_{Pi}^{\omega}\dot{P}_i$. In (22), the first term forces the consensus among DG units and second term causes the DGs to move toward the reference value. Equation (22) can be rewritten as

$$\dot{\delta}_{\omega i} = \alpha_{\omega}\sum_{j=1}^{N} a_{ij}\operatorname{sig}\left(\delta_{\omega j}-\delta_{\omega i}\right)^m + \beta_{\omega}\operatorname{sig}(\delta_{\omega i})^n, \quad t \geq t_{0f} \tag{23}$$

$$\dot{\delta}_{Pi} = \alpha_P\sum_{j=1}^{N} a_{ij}\operatorname{sig}\left(\delta_{Pj}-\delta_{Pi}\right)^q$$

Theorem 2: The control protocol designed in (22) solves the finite-time frequency restoration and active power-sharing problem in (3) with convergence time T_f.

Proof: Taking Lyapunov function as

$$V_2(t) = V_{\omega}(t) + V_P(t) = \frac{1}{2}\sum_{j=1}^{N}\delta_{\omega i}^2 + \frac{1}{2}\sum_{j=1}^{N}\delta_{Pi}^2 \tag{24}$$

Differentiating w.r.t. time (24) yields

$$\dot{V}_2(t) = \sum_{j=1}^{N}\delta_{\omega i}\dot{\delta}_{\omega i} + \sum_{j=1}^{N}\delta_{Pi}\dot{\delta}_{Pi} \tag{25}$$

Substituting (23) into (25), we get

$$\begin{aligned}\dot{V}_2(t) = &\sum_{j=1}^{N}\delta_{\omega i}\left(\alpha_{\omega}\sum_{j=1}^{N}a_{ij}\operatorname{sig}\left(\delta_{\omega j}-\delta_{\omega i}\right)^m + \beta_{\omega}\operatorname{sig}(\delta_{\omega i})^n\right)\\ &+\sum_{j=1}^{N}\delta_{Pi}\left(\alpha_P\sum_{j=1}^{N}a_{ij}\operatorname{sig}\left(\delta_{Pj}-\delta_{Pi}\right)^q\right), \quad t \geq t_{0f}\end{aligned} \tag{26}$$

Equation (26) can be rewritten as

$$\begin{aligned}\dot{V}_2(t) = &-\frac{1}{2}\sum_{j=1}^{N}\sum_{j=1}^{N}\left(\left(\alpha_{\omega}a_{ij}\right)^{2/(1+\alpha)}\left|\delta_{\omega j}-\delta_{\omega i}\right|^{2(1+m)/(1+\alpha)}\right)^{(1+\alpha)/2}\\ &-\sum_{j=1}^{N}\left(\beta_{\omega}^{2/(1+\alpha)}\left|\delta_{\omega i}\right|^{2(1+n)/(1+\alpha)}\right)^{(1+\alpha)/2}\\ &-\frac{1}{2}\sum_{j=1}^{N}\sum_{j=1}^{N}\left(\left(\alpha_P a_{ij}\right)^{2/(1+\alpha)}\left|\delta_{Pj}-\delta_{Pi}\right|^{2(1+q)/(1+\alpha)}\right)^{(1+\alpha)/2}\end{aligned} \tag{27}$$

where $0<\alpha<1$. By Lemma 3, (27) can be rewritten as

$$\begin{aligned}\dot{V}_2(t) \leq -\frac{1}{2}\Bigg(&\sum_{j=1}^{N}\sum_{j=1}^{N}\left(\alpha_{\omega}a_{ij}\right)^{2/(1+\alpha)}\left|\delta_{\omega j}-\delta_{\omega i}\right|^{2(1+m)/(1+\alpha)}\\ &+2\beta_{\omega}^{2/(1+\alpha)}\sum_{j=1}^{N}\left|\delta_{\omega i}\right|^{2(1+n)/(1+\alpha)}\Bigg)^{(1+\alpha)/2}\\ &-\frac{1}{2}\Bigg(\sum_{j=1}^{N}\sum_{j=1}^{N}\left(\alpha_P a_{ij}\right)^{2/(1+\alpha)}\left|\delta_{Pj}-\delta_{Pi}\right|^{2(1+q)/(1+\alpha)}\Bigg)^{(1+\alpha)/2}\end{aligned} \tag{28}$$

Define $\delta_{\omega}=[\delta_{\omega 1},\ldots\delta_{\omega N}]^{\mathrm{T}}$, and $\delta_P=[\delta_{P1},\ldots\delta_{PN}]^{\mathrm{T}}$, and

$$\begin{aligned}M_1(\delta_{\omega}) = &\sum_{j=1}^{N}\sum_{j=1}^{N}\left(\alpha_{\omega}a_{ij}\right)^{2/(1+\alpha)}\left|\delta_{\omega j}-\delta_{\omega i}\right|^{2(1+m)/(1+\alpha)}\\ &+2\beta_{\omega}^{2/(1+\alpha)}\sum_{j=1}^{N}\left|\delta_{\omega i}\right|^{2(1+n)/(1+\alpha)},\end{aligned}$$

$$\begin{aligned}M_2(\delta_{\omega}) = &\sum_{j=1}^{N}\sum_{j=1}^{N}\left(\alpha_{\omega}a_{ij}\right)^{2/(1+\alpha)}\left|\delta_{\omega j}-\delta_{\omega i}\right|^{2}\\ &+2\beta_{\omega}^{2/(1+\alpha)}\sum_{j=1}^{N}\left|\delta_{\omega i}\right|^{2}\end{aligned}$$

$$S_1(\delta_P) = \sum_{j=1}^{N}\sum_{j=1}^{N}\left(\alpha_P a_{ij}\right)^{2/(1+\alpha)}\left|\delta_{Pj}-\delta_{Pi}\right|^{2(1+q)/(1+\alpha)},$$

$$S_2(\delta_P) = \sum_{j=1}^{N}\sum_{j=1}^{N}\left(\alpha_P a_{ij}\right)^{2/(1+\alpha)}\left|\delta_{Pj}-\delta_{Pi}\right|^{2}$$

with $M_2(\delta_{\omega}), S_2(\delta_P)\neq 0$, because if M_2 and S_2 are zero then the connectivity of $G(\boldsymbol{A}_G)$, $\delta_i=\delta_j$, for all i,j and $V_2(t)=0$ which is contradictory. There M_2 and $S_2\neq 0$, and $M_1(\delta_{\omega})/M_2(\delta_{\omega})\geq k_{\omega}$ and $S_1(\delta_P)/S_2(\delta_P)\geq k_P$, where k_{ω} and $k_P>0$ and is given as

$$k_{\omega} = \frac{\min_{\substack{i,\,j\in N\\ a_{ij}\neq 0}}\left(\alpha_{\omega}a_{ij}\right)^{2/(1+\alpha)}\left(\delta_{\omega i}(0)-\delta_{\omega j}(0)\right)^{2(((1+m)/(1+\alpha))-1)}}{\sum_{i=1}^{N}\sum_{j=1}^{N}\left(\alpha_{\omega}a_{ij}\right)^{2/(1+\alpha)}}$$

$$k_P = \frac{\min_{\substack{i,\,j\in N\\ a_{ij}\neq 0}}\left(\alpha_P a_{ij}\right)^{2/(1+\alpha)}\left(\delta_{Pi}(0)-\delta_{Pj}(0)\right)^{2(((1+q)/(1+\alpha))-1)}}{\sum_{i=1}^{N}\sum_{j=1}^{N}\left(\alpha_P a_{ij}\right)^{2/(1+\alpha)}}$$

Following the process similar to [28], we can get:

$$\dot{V}_2(t) \le -\frac{1}{2}(4k_\omega\lambda_2(\mathrm{L}_\omega))^{(1+\alpha)/2}V_\omega(t)^{(1+\alpha)/2} - \frac{1}{2}(4k_P\lambda_2(L_P))^{(1+\alpha)/2}V_P(t)^{(1+\alpha)/2} \tag{29}$$

where $\lambda_2(L_\omega)$ and $\lambda_2(L_P)$ are the second smallest eigenvalues of the Laplacian matrices of the graphs G_ω and G_P with adjacency matrices $\boldsymbol{A}_\omega = [\alpha_\omega a_{ij}]^{2/(1+\alpha)}$ and $\boldsymbol{A}_P = [\alpha_P a_{ij}]^{2/(1+\alpha)}$, respectively. Thus, by using Lemma 4, $V_2(t)$ will reach zero in finite-time $T_f = \max\{t_\omega, t_P\}$, with

$$t_\omega \le \frac{2V_\omega(0)^{(1-\alpha)/2}}{(1-\alpha)(4k_\omega\lambda_2(L_\omega))^{(1+\alpha)/2}} \tag{30}$$

$$t_P \le \frac{2V_P(0)^{(1-\alpha)/2}}{(1-\alpha)(4P\lambda_2(L_P))^{(1+\alpha)/2}} \tag{31}$$

This completes the proof. □

Fig. 2 shows the control structure of the proposed secondary IDS-based frequency restoration scheme.

Remark 3: For larger MG network spanned over a large geographical area and MG clusters with few DGs or the leader DG of each group in the cluster must have the reference information to effectively restore the voltages and frequencies to their nominal values after sudden load disturbance. The proposed IDS can be used to estimate the reference information in a short time duration for all DGs present in the MG network. Thus, the proposed control scheme does not necessitate a complex bidirectional communication network and exhibits efficient performance with the cost-effective sparse communication network.

4 Finite-time distributed secondary voltage restoration

To exploit the advantage of the distributed control structure, the central controller is omitted. Therefore, only a subset of DGs has access to the voltage reference V_{ref}. Thus, an IDS similar to (5) is designed to provide voltage reference for each DG, and can be given as

$$\dot{r}_i = \mathrm{sig}\left(\sum_{j=1}^{N} a_{ij}(r_j - r_i) + c_i(V_{\mathrm{ref}} - r_i)\right)^{1/2} \tag{32}$$

where r_i will be the local estimate of the global information V_{ref}. Following the same procedure as that of Theorem 1, we can show that there exists a settling time t_{0V} such that $r_i = V_{\mathrm{ref}}$ as $t \ge t_{0V}$. Differentiating (2) w.r.t. yields

$$\dot{V}_{odi} = \dot{V}_i^d - k_{Qi}^V\dot{Q}_i = \varepsilon_i^V, \quad \dot{V}_i^d = \varepsilon_i^V + k_{Qi}^V\dot{Q}_i \tag{33}$$

$$V_i^d = \int\left(\varepsilon_i^V + k_{Qi}^V\dot{Q}_i\right)\mathrm{d}t \tag{34}$$

The auxiliary control input ε_i^V is designed as

$$\varepsilon_i^V = \alpha_V\sum_{j=1}^{N} a_{ij}\mathrm{sig}(V_{odj} - V_{odi})^m + \beta_V\mathrm{sig}(V_{\mathrm{ref}} - V_{odi})^n, \quad t \ge t_{0V} \tag{35}$$

where α_V and β_V are the coupling gains, $0 < m < 1$, and $n = 2m/(m+1)$.

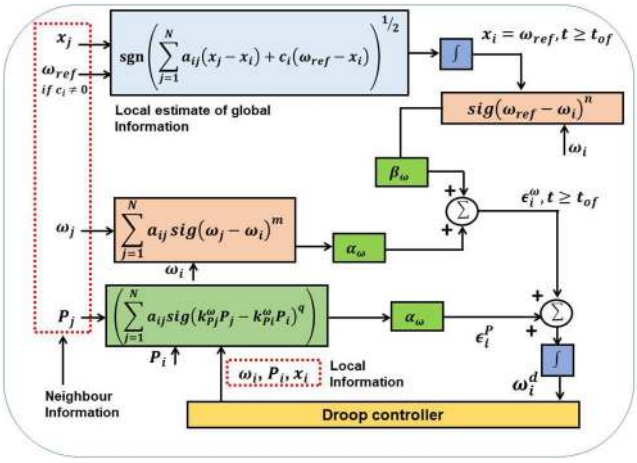

Fig. 2 *Proposed frequency restoration scheme*

Table 1 Specification of MG test system

DGs			
DG 1 & DG 2 & DG 3		DG 4 & DG 5	
k_Q^V	9.4×10^{-5}	k_Q^V	12.5×10^{-5}
k_P^ω	1.3×10^{-3}	k_P^ω	1.5×10^{-3}
R	0.03 Ω	R	0.03 Ω
L	0.35 mH	L	0.35 mH
R_f	0.1 Ω	R_f	0.1 Ω
L_f	1.35 mH	L_f	1.35 mH
C_f	50 μF	C_f	50 μF
K_{PV}	0.1	K_{PV}	0.05
K_{IV}	420	K_{IV}	390
K_{PC}	15	K_{PC}	10.5
K_{IC}	20,000	K_{IC}	16,000

Lines			
$Z_{\mathrm{Line}\,12}$	$Z_{\mathrm{Line}\,23}$	$Z_{\mathrm{Line}\,34}$	$Z_{\mathrm{Line}\,45}$
$R_l = 0.12\,\Omega$	$R_l = 0.175\,\Omega$	$R_l = 0.12\,\Omega$	$R_l = 0.175\,\Omega$
$L_l = 318\,\mu\mathrm{H}$	$L_l = 1847\,\mu\mathrm{H}$	$L_l = 318\,\mu\mathrm{H}$	$L_l = 1847\,\mu\mathrm{H}$

Theorem 3: Let the communication topology be connected, then the control protocol designed in (4) solves the finite-time voltage restoration problem in (4) with convergence time

$$T_V \le \frac{2V_3(0)^{(1-\alpha)/2}}{(1-\alpha)(4k_V\lambda_2(L_V))^{(1+\alpha)/2}} \tag{36}$$

where $\lambda_2(L_V)$ is the second smallest eigenvalue of Laplacian matrix of graph G_V with adjacency matrices $\boldsymbol{A}_V = [\alpha_V a_{ij}]^{2/(1+\alpha)}$, and $V_3(t)$ is the Lyapunov function.

Proof: The proof is similar to the proof in Theorem 2. □

5 Simulation results

In this section, an islanded three phase, inverter-based AC MG test system (380 V per phase RMS, 50 Hz) is simulated under different scenarios in MATLAB/SimPowerSystem environment. The solver used is ode45 (Dormand–Prince) with relative tolerance of 1×10^{-6} and variable step. The considered MG test system includes five DG units and five local loads. The loads and lines are modelled as series RL branches. The detailed MG specification, loads, and proposed controller parameters are summarised in Tables 1–3, respectively. The DG units communicate over a sparse communication network that forms a weighted graph. Fig. 3 shows

Table 2 MG loads

Loads				
Load 1	Load 2	Load 3	Load 4	Load 5
$R = 300\,\Omega$	$R = 40\,\Omega$	$R = 50\,\Omega$	$R = 40\,\Omega$	$R = 50\,\Omega$
$L = 477$ mH	$L = 64$ mH	$L = 64$ mH	$L = 64$ mH	$L = 95$ mH

Table 3 Parameters of proposed algorithm

Voltage controller	Frequency controller	Active power controller	Reference
$\alpha_V = 200$	$\alpha_\omega = 80$	$\alpha_P = 100$	$V_{\text{ref}} = 380$ V
$\beta_V = 100$	$\beta_\omega = 40$	$q = 1/3$	$f_{\text{ref}} = 50$ Hz
$m = 1/3$	$m = 1/3$	$\alpha = 0.5$	—
$n = 1/2$	$n = 1/2$	—	—
$\alpha = 0.5$	$\alpha = 0.5$	—	—

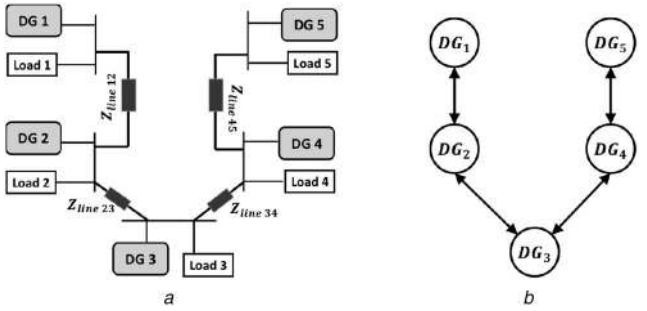

Fig. 3 *Simulated MG network*
(a) Islanded MG test system, ***(b)*** Communication topology

the single line diagram of the MG test system and considered communication topology.

5.1 Performance under load variation

Here, we present the effectiveness of the proposed secondary control scheme after islanding takes place at $t = 0$ s. The primary control and IDS are active whereas the secondary control is intentionally deactivated. The primary control results in voltage and frequency deviations from reference values. Therefore, secondary control in (21) and (34) are activated at $t = 1$ s, the voltage and frequency both are quickly restored to their reference values $V_{\text{ref}} = 380$ V, $f_{\text{ref}} = 50$ Hz, respectively with finite-time 0.22 s. Next, an additional RL load of $R = 30\,\Omega, L = 47$ mH is added to DG4 at $t = 2$ s, and is disconnected at $t = 3.5$ s. Figs. 4*a* and *b* show that, the secondary control effectively rejects the load disturbances and restores the voltage and frequency with small transients in finite-time.

Further Fig. 4*c* shows the accurate active power-sharing among all the DGs throughout the run time according to their rating, i.e. $P_1{:}P_2{:}P_3{:}P_4{:}P_5 = (1/k_{P1}^{\omega}){:}(1/k_{P2}^{\omega}){:}(1/k_{P3}^{\omega}){:}(1/k_{P4}^{\omega}){:}(1/k_{P5}^{\omega})$.

5.2 Performance under time-varying communication topologies

In a practical scenario, the DGs share information over a communication digraph which depends on their geographical locations. To replicate this scenario, the proposed controller is implemented under a time-varying communication topology as shown in Fig. 5. Consider digraph $T_G = \{G_a, G_b, G_c, G_d\}$, where DG1 has direct access to the reference value with $c_1 = 1$. Considering G_a as the initial communication topology and it switches to next topology at every $t = 0.5$ s in cycle the $G_a \to G_b \to G_c \to G_d \to G_a$. At $t = 2$ s, load is connected to DG4 and detached at $t = 3.5$ s. As shown in Figs. 6*a* and *b*, the restoration time of the DGs voltage and frequency is increased marginally from 0.22 to 0.3 s as that of case 1, while maintaining precise active power-sharing shown in Fig. 6*c*. Therefore, the

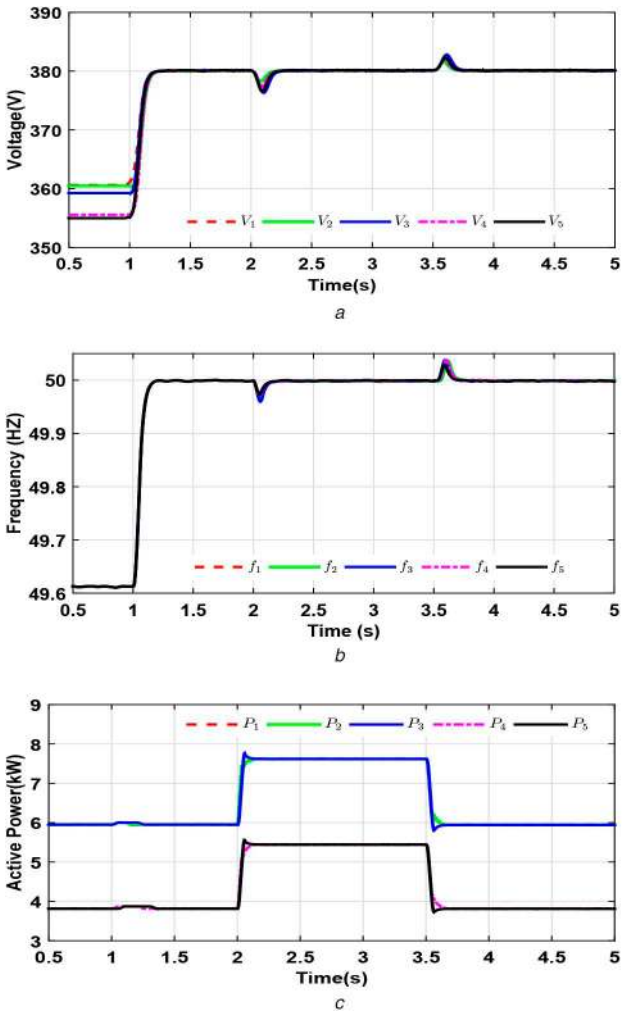

Fig. 4 *Performance of the proposed control under load variation*
(a) DG output voltage magnitude, ***(b)*** DG frequency, ***(c)*** DG output active power

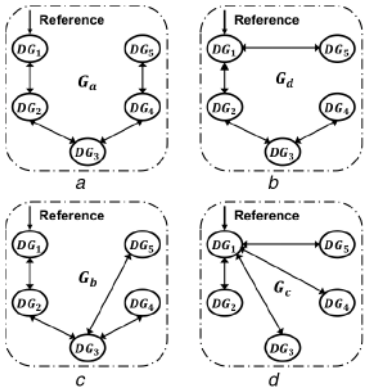

Fig. 5 *Digraph of time-varying communication topology*
(a) Communication topology G_a, ***(b)*** Communication topology G_b, ***(c)*** Communication topology G_c, ***(d)*** Communication topology G_d

performance of the proposed controller is fairly acceptable regardless of time-varying communication topology.

5.3 Performance under PNP capability

The intermittent nature of renewable generation demands the control scheme that supports the PNP capability of MG. In this case, PNP capability of the proposed controller is analysed by disconnecting DG5 at $t = 3$ s, and connecting back at $t = 4$ s. Failure of one DG unit results in communication link breakage of that unit, i.e. disconnection of DG5 results in communication link 4-5 breakage. The existing communication links still form a connected graph. Fig. 7*c* shows that at $t = 3$ s, DG5 disconnects

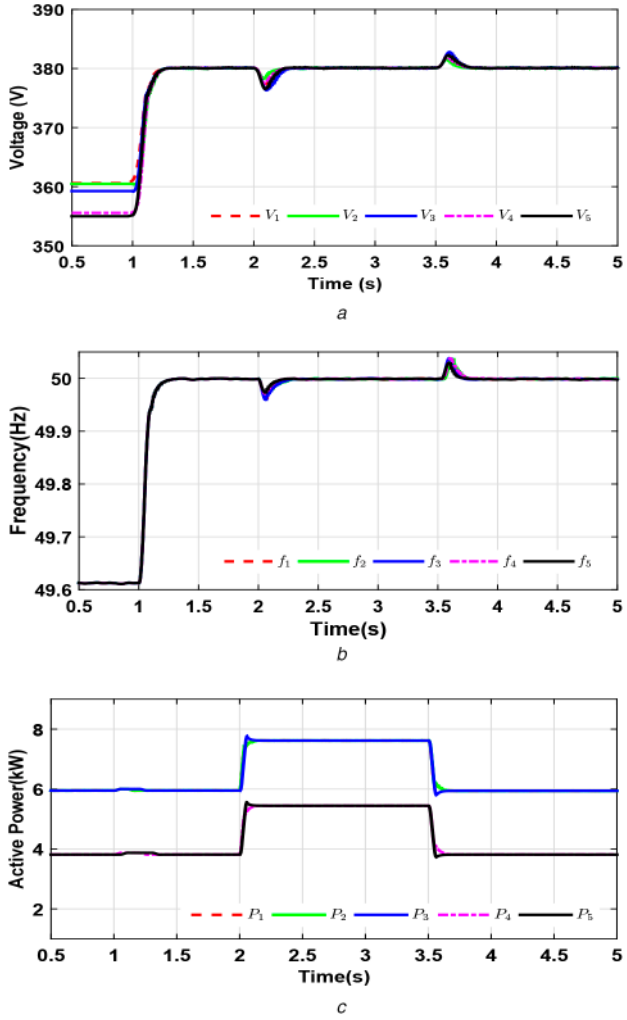

Fig. 6 *Performance of the proposed control under time-varying communication topology*
(a) DG output voltage magnitude, ***(b)*** DG frequency, ***(c)*** DG output active power

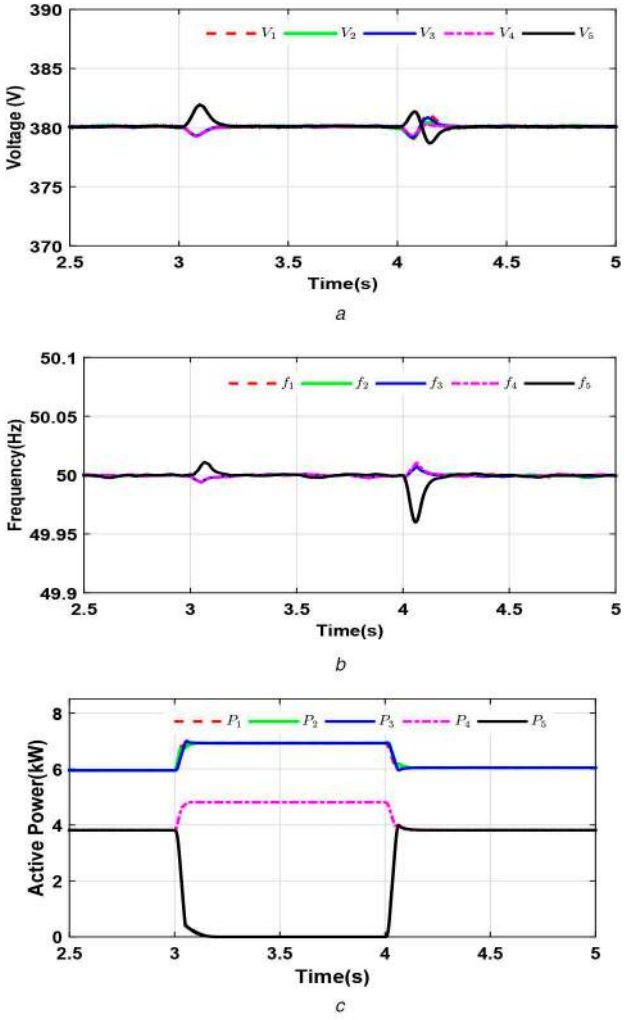

Fig. 7 *Performance of the proposed control for PNP operation*
(a) DG output voltage magnitude, ***(b)*** DG frequency, ***(c)*** DG output active power

and remaining four DGs compensates for the power deficiency by increasing their output power. The output power of DG5 drops to zero with slow slope because the low-pass filter helps in harmonics rejection. Further, at $t = 4$ s, the communication topology is revised when DG5 is reconnected to MG as shown in Fig. 8. Fig. 7 shows that the voltage, frequency, and active power regulation are maintained seamlessly with small transient at disconnection and re-connection points, and proposed control scheme supports the PNP demand of MG.

5.4 Comparative performance evaluation

A few studies in [9, 12, 26] consider both voltage and frequency restoration simultaneously. Therefore, to show the faster convergence, the proposed control scheme is compared with the conventional approach in [9, 26]. The controller in [9, 26] is asymptotic controller with exponential convergence rate whereas in this paper, the proposed control schemes for voltage, frequency, and active power tracking in (21) and (34), restores them to the reference values in finite-time, respectively. Fig. 9 shows that proposed method exhibits faster convergence and accurate performance for controller activation and load variation. For controller activation and sudden load change, the proposed controller restores the voltage in 0.2 and 0.19 s, respectively, whereas, the conventional asymptotic controller converges at 0.32 and 0.29 s, respectively. However, using higher controller gains the asymptotic methods may achieve similar performance, but results in high-frequency dynamics. For simplicity, the response of only DG1 is depicted. For simulation, we consider the same DG, line and loads parameters.

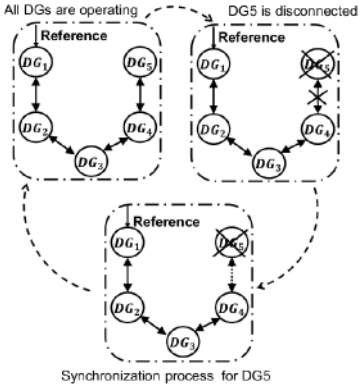

Fig. 8 *Digraph of communication topology in PNP case*

5.5 Effect of communication link delay

Communication is an important component of the proposed IDS-based secondary control scheme. Therefore, the effect of communication link delay is illustrated in this case. Here, three different communication delays $\tau = 0.1, 1$ and 2 s have been considered. The secondary control is activated at $t = 2$ s, and the restoration process starts for all DG units. For clarity, responses of only one DG unit are shown under different delays as given in Figs. 10 and 11. It is clear from Figs. 10*a* and *b* that the proposed controller effectively restores the voltage and frequency with a small time delay of 100 ms. Figs. 10*c* and *d* show that when the time delay τ is increased to 1 s, the voltage/frequency are restored with a small variation. However, the settling time is increased. Further, when the delay continues to increase to 2 s, the proposed

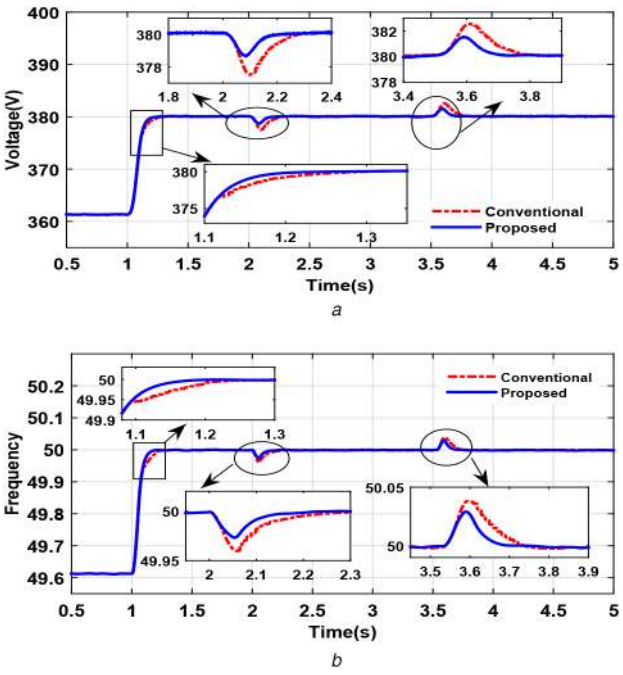

Fig. 9 *Comparison between proposed finite-time controller and asymptotic controller in [26]*
(a) DG output voltage magnitude, ***(b)*** DG frequency

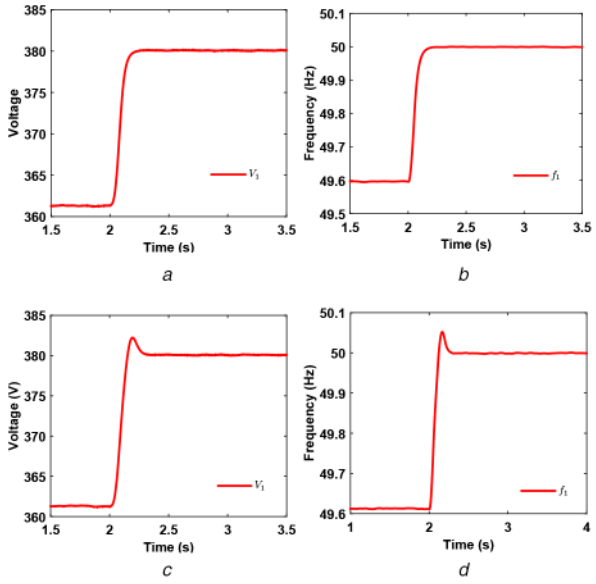

Fig. 10 *Performance under communication link delay*
(a) DG output voltage magnitude for $\tau_d = 100$ ms, ***(b)*** DG frequency for $\tau_d = 100$ ms, ***(c)*** DG output voltage magnitude for $\tau_d = 1$ s, ***(d)*** DG frequency for $\tau_d = 1$ s

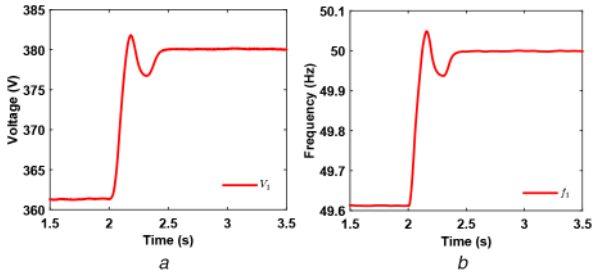

Fig. 11 *Performance under communication link delay*
(a) DG output voltage magnitude for $\tau_d = 2$ s, ***(b)*** DG frequency for $\tau_d = 2$ s

controller restores the voltage and frequency with higher settling time as seen in Fig. 11. Hence, it is clear that the communication link delay increases the setting time of the controller.

6 Conclusion

This paper focuses on the secondary control problem for voltage, frequency, and active power regulation in an islanded MG. In comparison with the conventional centralised control approach, the proposed method is fully distributed and reduces the computational burden and risk of single-point-failure. Since all the DG units do not have access to the voltage and frequency reference, an IDS is developed for each DG unit to provide the local estimate of global voltage and frequency references in finite-time. This information is further used to design the finite-time distributed secondary voltage and frequency restoration and active power-sharing scheme. Lyapunov proofs for finite-time restoration is provided along with the upper bound on convergence time. From the simulation results, the effectiveness of the proposed control scheme is verified under sudden load disturbances, time-varying communication topology, and PNP capability. The comparison between asymptotic control algorithm and the proposed control scheme shows that the proposed method improves the convergence speed and has better disturbance rejection.

7 References

[1] Lasseter, R.H.: 'Microgrids'. Power Engineering Society Winter Meeting, 2002, vol. 1, pp. 305–308

[2] Katiraei, F., Iravani, M.R., Lehn, P.W.: 'Micro-grid autonomous operation during and subsequent to islanding process', *IEEE Trans. Power Deliv.*, 2005, **20**, (1), pp. 248–257

[3] Guerrero, J.M., Vasquez, J.C., Matas, J., *et al.*: 'Hierarchical control of droop-controlled AC and DC microgrids – a general approach toward standardization', *IEEE Trans. Ind. Electron.*, 2011, **58**, (1), pp. 158–172

[4] Bidram, A., Davoudi, A.: 'Hierarchical structure of microgrids control system', *IEEE Trans. Smart Grid*, 2012, **3**, (4), pp. 1963–1976

[5] Pogaku, N., Prodanovic, M., Green, T.C.: 'Modeling, analysis and testing of autonomous operation of an inverter-based microgrid', *IEEE Trans. Power Electron.*, 2007, **22**, (2), pp. 613–625

[6] Savaghebi, M., Jalilian, A., Vasquez, J.C., *et al.*: 'Secondary control scheme for voltage unbalance compensation in an islanded droop-controlled microgrid', *IEEE Trans. Smart Grid*, 2012, **3**, (2), pp. 797–807

[7] Tan, K., Peng, X., So, P.L., *et al.*: 'Centralized control for parallel operation of distributed generation inverters in microgrids', *IEEE Trans. Smart Grid*, 2012, **3**, (4), pp. 1977–1987

[8] Vovos, P.N., Kiprakis, A.E., Wallace, A.R., *et al.*: 'Centralized and distributed voltage control: impact on distributed generation penetration', *IEEE Trans. Power Syst.*, 2007, **22**, (1), pp. 476–483

[9] Bidram, A., Davoudi, A., Lewis, F.L., *et al.*: 'Distributed cooperative secondary control of microgrids using feedback linearization', *IEEE Trans. Power Syst.*, 2013, **28**, (3), pp. 3462–3470

[10] Schiffer, J., Seel, T., Raisch, J., *et al.*: 'Voltage stability and reactive power sharing in inverter-based microgrids with consensus-based distributed voltage control', *IEEE Trans. Control Syst. Technol.*, 2016, **24**, (1), pp. 96–109

[11] Ahumada, C., Cárdenas, R., Sáez, D., *et al.*: 'Secondary control strategies for frequency restoration in islanded microgrids with consideration of communication delays', *IEEE Trans. Smart Grid*, 2016, **7**, (3), pp. 1430–1441

[12] Guo, F., Wen, C., Mao, J., *et al.*: 'Distributed secondary voltage and frequency restoration control of droop-controlled inverter-based microgrids', *IEEE Trans. Ind. Electron.*, 2015, **62**, (7), pp. 4355–4364

[13] Shafiee, Q., Guerrero, J.M., Vasquez, J.C.: 'Distributed secondary control for islanded microgrids – a novel approach', *IEEE Trans. Power Electron.*, 2014, **29**, (2), pp. 1018–1031

[14] Simpson-Porco, J.W., Shafiee, Q., Dörfler, F., *et al.*: 'Secondary frequency and voltage control of islanded microgrids via distributed averaging', *IEEE Trans. Ind. Electron.*, 2015, **62**, (11), pp. 7025–7038

[15] Nasirian, V., Shafiee, Q., Guerrero, J.M., *et al.*: 'Droop-free distributed control for AC microgrids', *IEEE Trans. Power Electron.*, 2016, **31**, (2), pp. 1600–1617

[16] Bidram, A., Davoudi, A., Lewis, F.L.: 'Finite-time frequency synchronization in microgrids'. 2014 IEEE Energy Conversion Congress and Exposition (ECCE), Pittsburgh, PA, USA, 2014, pp. 2648–2654

[17] Cady, S.T., Domnguez-Garca, A.D., Hadjicostis, C.N.: 'Finite-time approximate consensus and its application to distributed frequency regulation in islanded AC microgrids'. 2015 48th Hawaii Int. Conf. on System Sciences (HICSS), Hawaii, USA, 2015, pp. 2664–2670

[18] Zuo, S., Davoudi, A., Song, Y., *et al.*: 'Distributed finite-time voltage and frequency restoration in islanded AC microgrids', *IEEE Trans. Ind. Electron.*, 2016, **63**, (10), pp. 5988–5997

[19] Wang, X., Zhang, H., Li, C.: 'Distributed finite-time cooperative control of droop-controlled microgrids under switching topology', *IET Renew. Power Gener.*, 2016, **11**, (5), pp. 707–714

[20] Lou, G., Gu, W., Xu, Y., *et al.*: 'Distributed MPC-based secondary voltage control scheme for autonomous droop-controlled microgrids', *IEEE Trans. Sustain. Energy*, 2017, **8**, (2), pp. 792–804

[21] Shrivastava, S., Subudhi, B., Das, S.: 'Distributed voltage and frequency synchronisation control scheme for islanded inverter-based microgrid', *IET Smart Grid*, 2018, **1**, (2), pp. 48–56

[22] Meng, W., Wang, X., Liu, S.: 'Distributed load sharing of an inverter-based microgrid with reduced communication', *IEEE Trans. Smart Grid*, 2018, **9**, (2), pp. 1354–1364
[23] Lu, X., Yu, X., Lai, J.*, et al.*: 'A novel distributed secondary coordination control approach for islanded microgrids', *IEEE Trans. Smart Grid*, 2018, **9**, (4), pp. 2726–2740
[24] Deng, Z., Xu, Y., Sun, H.*, et al.*: 'Distributed, bounded and finite-time convergence secondary frequency control in an autonomous microgrid', *IEEE Trans. Smart Grid*, 2019, **10**, (3), pp. 2776–2788
[25] Xu, Y., Sun, H.: 'Distributed finite-time convergence control of an islanded low-voltage AC microgrid', *IEEE Trans. Power Syst.*, 2018, **33**, (3), pp. 2339–2348
[26] Bidram, A., Davoudi, A., Lewis, F.L.*, et al.*: 'Secondary control of microgrids based on distributed cooperative control of multi-agent systems', *IET Gener. Transm. Distrib.*, 2013, **7**, (8), pp. 822–831
[27] Olfati-Saber, R., Murray, R.M.: 'Consensus problems in networks of agents with switching topology and time-delays', *IEEE Trans. Autom. Control*, 2004, **49**, (9), pp. 1520–1533
[28] Wang, L., Xiao, F.: 'Finite-time consensus problems for networks of dynamic agents', *IEEE Trans. Autom. Control*, 2010, **55**, (4), pp. 950–955
[29] Hardy, G.H., Littlewood, J.E., Pólya, G.: '*Inequalities*' (Cambridge University Press, UK, 1952)
[30] Bhat, S.P., Bernstein, D.S.: 'Continuous finite-time stabilization of the translational and rotational double integrators', *IEEE Trans. Autom. Control*, 1998, **43**, (5), pp. 678–682